Statistical Analysis of Reactions Induced with 21–63 MeV Li⁶ Ions on Fe⁵⁴: Effects of Angular Momentum and Closed Shells on Nuclear Level Densities*

MARSHALL BLANN

Department of Chemistry, University of Rochester, Rochester, New York

(Received 25 September 1963)

Two sets of statistical theory calculations have been compared with experimental excitation functions for the production of Ni^{56}, Ni^{57}, Co^{56}, Co^{57}, Mn^{54}, and Fe^{52} at excitation energies up to 70 MeV. The reactions were induced with Li^6 ions on Fe^{54}. The first set of calculations was based on the assumption that $\rho(E,J) = C(2J+1)\rho(E)$, where $\rho(E) = C'E^{-2}\exp2(aE)^{1/2}$. The excitation energy E was corrected for pairing, a was taken equal to 7.0 MeV^{-1} as determined from (p,α) and (α,α') spectra, and optical-model nonelastic cross sections were used for inverse reaction cross sections. All permutations of n, p, d, t, He^3, and α emission were calculated for the first two particles out, followed by all permutations of n, p, and α emission for further evaporation. The excitation functions so calculated were narrower, and peaked at lower excitation energies than the experimental excitation functions. A second set of calculations was made assuming $\rho(E,J)$ $= C'(2J+1)\rho(E-\bar{E}_{\text{rotational}})$, where the average rotational energy, assumed to remain constant throughout the series of intermediate nuclei involved in a particle emission cascade, was calculated with the use of optical-model transmission coefficients for Li^6 ions incident on Fe^{54}. Excitation functions calculated with the latter assumption are in excellent agreement with experimental values with respect to width and excitation energy of maxima. Neither set of calculations is in good agreement with experimental values with respect to magnitude of maxima. It is suggested that these discrepancies may partially be explained as due to the influence of the 28-neutron and 28-proton shells on nuclear level densities.

I. INTRODUCTION

THE compound-nucleus and statistical models of nuclear reactions are at present well established, well documented, and adequately reviewed.[1–3] There are nontheless many open questions with respect to the statistical model. One of these is the range of excitations over which nuclei may be considered to have attained statistical equilibrium. Reactions leading to formation of highly excited nuclei usually lead also to states of considerable angular momentum. Thus, a consideration of upper excitation energy limits for statistical equilibrium necessarily requires a simultaneous consideration of effects of angular momentum on nuclear level densities. The motivation for this work was to partially answer the above two questions.

In a previous statistical analysis of the decay of Cu^{60} nuclei (resulting from deuteron bombardment of Ni^{58}) at excitation energies of 14–34 MeV, it was shown that the theoretical predictions agreed well with experimental results.[4] In the preceding paper the range of excitation energy was extended to 70.4 MeV by bombardment of Fe^{54} with 21–63-MeV Li^6 ions.[5] It was shown that excitation functions for the production of Ni^{56}, Ni^{57}, Co^{56}, Co^{57}, Mn^{54}, and Fe^{52} are consistent with a compound-nucleus mechanism, with Cu^{60} the compound nucleus. We propose here to extend the statistical calculations to an excitation energy of 70 MeV, employing the independently determined parameters that were

found to fit the deuteron excitation function data in the lower energy range. A rotational energy correction is to be applied in calculating density of states, and calculations with and without rotational energy corrections will be compared with experimental results to see if experimental excitation functions are still consistent with statistical equilibrium, and to see the change introduced by the adjustment for rotational energy. The rotational correction used was selected for simplicity and is, in most polite terms, less than rigorous.

An additional point of interest in this investigation lies in the possible effects of the 28-nucleon closed shell on nuclear level densities. While nonequilibrium and rotational energy effects may tend to move excitation functions to higher energies, shell effects on level densities should be reflected as changes in relative cross sections. The singly closed-shell Ni^{57} nucleus and doubly closed-shell Ni^{56} nucleus apparently show such an effect. To rule out the possibility that this effect is due solely to the difference in neutron and proton binding energies one must perform a statistical-model analysis. If the yields of the nickel isotopes are still anomalously low, and if the reaction actually proceeds by a compound-nucleus mechanism, a probable explanation is that the 28-nucleon shell does indeed influence level densities of highly excited nuclei. This possibility will also be investigated.

II. EVAPORATION CALCULATIONS

A. Theory

The calculations in this paper are based on the statistical theory of nuclear reactions.[6–9] A frequently used

[1] H. Feshbach, in *Nuclear Spectroscopy*, edited by F. Ajzenberg-Selove (Academic Press Inc., New York, 1960), Part B.

[2] T. Erickson, in *Advances in Physics*, edited by N. F. Mott (Taylor and Francis, Ltd., London, 1960), Vol. 9, p. 425.

[3] D. Bodansky, in *Annual Reviews of Nuclear Science* (Annual Reviews, Inc., Palo Alto, California, 1962), Vol. 12.

[4] M. Blann and G. Merkel, Phys. Rev. **131**, 764 (1963).

[5] M. Blann, F. M. Lanzafame, and R. A. Piscitelli, Phys. Rev. **133**, B700 (1964), preceding paper.

[6] V. F. Weisskopf, Phys. Rev. **52**, 295 (1937).

[7] L. Wolfenstein, Phys. Rev. **92**, 690 (1951).

[8] T. Ericson and V. Strutinski, Nucl. Phys. **8**, 284 (1958).

[9] A. M. Lane and R. G. Thomas, Rev. Mod. Phys. **30,**257 (1958).

formulation has been used,[6] i.e., we have assumed that

$$P_i(E^*,\epsilon)d\epsilon = \gamma_i \sigma_{\mathrm{inv}}(E,\epsilon)\frac{\rho(E)}{\rho(E^*)}\epsilon d\epsilon, \qquad (1)$$

where $P_i(E^*,\epsilon)$ represents the probability per unit time that a nucleus at excitation E^* will emit a particle i with channel energy between ϵ and $\epsilon + d\epsilon$; $\gamma_i = g_i m_i/\pi^2\hbar^3$, where g_i is the number of spin states of particle i and m_i is the reduced mass of particle i. The expression $\rho(E)/\rho(E^*)$ is the ratio of the level densities of final to initial nuclei. The inverse cross section $\sigma_{\mathrm{inv}}(E,\epsilon)$ is the cross section for the capture of particle i with kinetic energy between ϵ and $\epsilon + d\epsilon$ by the residual nucleus at excitation E to form the initial nucleus with excitation E^*.

In the derivation of Eq. (1) it is necessary to assume that there are no angular-momentum-conservation restrictions on the decay of the compound nuclei,[2,10] which is equivalent to the assumption that

$$\rho(E,J) = C(2J+1)\rho(E). \qquad (2)$$

If the conservation of angular momentum is imposed, Eq. (2) becomes[2,3]

$$\rho(E,J) = \frac{(2J+1)}{2(2\pi)^{1/2}\sigma^3}\rho(E)\exp[-J(J+1)/2\sigma^2], \quad (3)$$

where σ^2 is the mean-square projection of the nuclear angular momentum on a fixed axis and is itself a function of excitation energy.[11-13]

Use of Eq. (3) to calculate particle emission probabilities is extremely tedious relative to use of Eq. (2), since, in the former instance, calculations require use of individual transmission coefficients, and in the latter case a great simplification results whereby Eq. (1) is valid using inverse reaction cross sections, where σ_{inv} is related to the transmission coefficients by[3]

$$\sigma_{\mathrm{inv}}(\epsilon) = \pi\lambda^2 \sum_{l=0}^{\infty}(2l+1)T_l(\epsilon). \qquad (4)$$

Because of the great simplication noted above for use of Eq. (1) assuming the validity of Eq. (2), several computer programs were written to integrate Eq. (1) for multiple particle emission. Excitation functions were calculated for decay of Cu^{60} nuclei at excitation energies from 14 to 70 MeV. Optical-model calculations show that l waves up to $24\hbar$ make significant contributions to

the formation of these Cu^{60} compound nuclei.[14] Under these conditions use of Eq. (2) is surely not justified; one wishes to know what change would result from the use of Eq. (3). In the following paragraphs we shall qualitatively discuss the differences of an evaporation calculation using Eq. (3) rather than Eq. (2). We shall try to show that where only single nucleons are emitted in an evaporation cascade, Eq. (2) may be used with an average rotational energy correction as a first approximation to Eq. (3). The application of such an average rotational energy correction will be made to the initial compound nucleus and to all the intermediate nuclei in an evaporation cascade in the calculations to follow (those for which we claim a rotational energy correction has been made). The rotational energy correction will vary in magnitude with the initial excitation energy, as the incoming Li^6 ion brings in more or less angular momentum (as calculated with the optical model).

The advantages of using Eq. (3) rather than Eq. (2) in evaporation calculations may be roughly grouped into two categories. First, application of Eq. (3) yields the level density in the E,J plane rather than in just the E plane, and is therefore useful in determining E_J, the lowest excitation energy having an available state of spin J. This in turn permits calculation of gamma-ray de-excitation probability as based on the following argument.[15] Near the end of the evaporation cascade the residual nucleus has high angular momentum and low excitation energy. The next nucleon, if it is to be emitted, must either carry off a very high angular momentum or alternatively find a high-spin, low-excitation state to decay to. Since single nucleons emitted at low kinetic energy are limited in the amount of angular momentum they can remove, and since there is usually a scarcity of high-spin states near ground, the particle either cannot be emitted or spends a long time "looking" for a suitable state. In either case, gamma-ray de-excitation would be enhanced.

The second main change resulting from use of Eq. (3) rather than Eq. (2) is in calculating the change in level density as a function of the angular momentum carried off by the out going particle. An evaporated neutron or proton will, on the average, carry off less than one unit of angular momentum. Thus, the exponential of Eq. (3) will show little change during the emission cascade of neutrons and protons (assuming a constant nuclear moment of inertia throughout the cascade)[16] and Eq. (3) will reduce in form to Eq. (2). If, however, complex particles (e.g., α particles) make significant contributions to the evaporation process, the exponential of Eq. (3) may show considerable change as the emitted particle carries off several units of angular momentum.

[10] G. R. Satchler, in Proceedings of the Conference on Reactions Between Complex Nuclei, Gatlinburg [Oak Ridge National Laboratory Report ORNL-2606, 1958 (unpublished)], p. 79.

[11] G. Merkel, University of California Lawrence Radiation Laboratory Report UCRL-9898, 1962 (unpublished).

[12] H. W. Fulbright, N. O. Lassen, and N. O. Roy Poulsen, Kgl. Danske Videnskab. Selskab, Mat. Fys. Medd. 31, No. 10 (1959).

[13] J. Benveniste, G. Merkel, and A. Mitchell, Bull. Am. Phys. Soc. 7, 454 (1962).

[14] The optical-model program due to Bjorklund and Fernbach was used for the $Fe^{54}+Li^6$ calculation. Parameters used are listed in Table I.

[15] J. R. Grover, Phys. Rev. 127, 2142 (1962).

[16] M. S. Halbert and F. E. Durham, Third Conference on Reactions Between Complex Nuclei, Asilomar, April 1963 (unpublished).

Such a change would affect the relative emission probabilities of nucleons and complex particles, and should result in a change in relative magnitude of the excitation functions. The first effect discussed (in the preceding paragraph) should be manifested as a shift in energy of the excitation function. In this work we are mainly concerned with reactions in which neutrons and protons are the predominant emitted species, and are therefore concerned with the first mentioned property of Eq. (3).

It has been shown that the exponent of the spin cutoff may be considered as resulting from energy tied up as classical rotational energy,[2,3] and therefore not available for exciting intrinsic states. With this orientation the effect of the spin cutoff term may to a first approximation be taken into account by decreasing the excitation energy by an amount equal to the average classical rotational energy

$$\bar{E}_{\text{rot}} = \frac{\left[\sum\limits_{l=0}^{\infty} (2l+1)T_l(l)(l+1)\hbar^2/2\mathscr{I}_{\text{rigid}}\right]}{\sum\limits_{l=0}^{\infty} (2l+1)T_l}, \quad (5)$$

giving

$$\rho(E,J) \propto (2J+1)\rho(E-\bar{E}_{\text{rot}}), \quad (6)$$

and this approximation should be a reasonable first approximation to Eq. (3) as long as J and σ remain constant, and E is not too low compared with the rotational energy. The approximation of Eq. (6) has been used in this work. With this approximation Eq. (1) is still valid. We further assume that the energy committed to rotation eventually is dissipated as γ radiation, i.e., is not available for particle emission. We emphasize that the averaging indicated in Eq. (5) as subsequently used in Eq. (6) does not give the same weighting as an actual calculation using Eq. (3) with transmission coefficients. We nonetheless use this as a first approximation to gain insight into the more complex problem.

In these calculations we have used a Fermi-gas level density of the form[17–19]

$$\rho(E) = CE^{-2}\exp2(aE)^{1/2}, \quad (7)$$

where C is a constant, independent of the even or odd character of nuclei. Odd-even effects on the nuclear level densities have been taken into consideration by a displacement in the ground-state energy,[20]

$$\rho(E) = C(E-\delta)^{-2}\exp2[a(E-\delta)]^{1/2}; \quad (8)$$

where the rotational energy correction is applied, the excitation energy used in Eq. (8) becomes $E-\delta-\bar{E}_{\text{rot}}$.

The parameters of Eqs. (1) and (8) must be evaluated before proceeding with an actual calculation of excitation functions. We wish to use the best set of independently determined parameters available.

B. Parameters

1. Level Density Parameter

The value of a used in Eq. (8) was 7.0 MeV⁻¹. This value was determined from Ni⁵⁸(p,α) particle spectra by Brady and Sherr[21] and from Fe⁵⁶ (α,α') spectra by Benveniste et al.[13] The incident protons were 15.6 and 19.4 MeV; the incident alpha particles were 21 MeV.

2. Pairing Correction

The ground-state energy shift was assumed to be equal to the pairing energy. The values used were taken as half the difference between M-A versus Z plots for even-A nuclides in the $A=60$ region. The following values were found: for odd-A nuclides, $\delta = 1.4$ MeV, for odd-odd nuclides $\delta = 0$ MeV, and for even-even nuclides $\delta = 2.8$ MeV.[22]

3. Inverse Reaction Cross Sections

Values of inverse reaction cross sections are obviously not available. It has been customary in statistical-model analyses to use instead ground-state capture cross sections, i.e., assume

$$\sigma_{\text{inv}}(0,\epsilon) = \sigma_{\text{inv}}(E,\epsilon). \quad (9)$$

Values of $\sigma(0,\epsilon)$ used in this work were optical-model total nonelastic cross sections. Optical-model parameters were selected from elastic scattering results, where available. An exception to this statement was the calculation of neutron nonelastic cross sections. The neutron optical-model parameters from elastic scattering correspond to a reasonably transparent nucleus; since the nuclei studied in this work are highly excited they should be more opaque than nuclei in their ground state, as a consequence of the Pauli exclusion principle.[2] For this reason the imaginary potential well was arbitrarily deepened for low-energy neutrons. The optical-model parameters used in calculating nonelastic cross sections used in this work are summarized in Table I.

4. Average Rotational Energy

One of the two sets of calculations of this work was performed assuming the validity of Eq. (6), as previously stated. The rotational energy to be subtracted was calculated as an average rotational energy, as given by Eq. (5), where the transmission coefficients were calculated with the nuclear optical model (Table I) and $\mathscr{I}_{\text{rigid}}$ (the rigid body moment of inertia) was calcu-

[17] H. A. Bethe, Rev. Mod. Phys. 9, 69 (1937).
[18] T. Ericson, in Proceedings of the International Conference on Nuclear Structure, Kingston Canada, 1960, edited by D. A. Bromley and E. Vogt (University of Toronto Press, Toronto, 1960), p. 697.
[19] D. W. Lang, Nucl. Phys. 26, 434 (1961).
[20] H. Hurwitz and H. Bethe, Phys. Rev. 81, 898 (1951).

[21] F. P. Brady and R. Sherr, Phys. Rev. 124, 1928 (1961).
[22] F. Everling, L. A. Konig, J. H. E. Mattauch, and A. H. Wapstra, Nucl. Phys. 18, 529 (1960).

TABLE I. Summary of optical-model parameters used in calculating nonelastic cross sections.

Incident particle	Radius parameter (F)	Projectile size (F)	Diffuseness parameter (F)	Real potential depth (MeV)	Imaginary potential depth (MeV)	Type of absorption	Reference to source of parameters and general details not listed in table
n	1.25	0	a	52	20	Gaussian surface	a
p	1.25	0	not constant[a]			Gaussian surface	a
α	1.14	2.24	0.50	49.3	11	volume	a
d	1.14	1.20	0.50	50	20	volume	b
t	1.14	2.24	0.50	50	20	volume	b
He³	1.14	2.24	0.50	50	20	volume	b
Li⁶	1.14	1.20	0.50	50	20	volume	b

[a] F. E. Bjorklund and S. Fernbach, in Proc. Intern. Conf. Peaceful Uses At. Energy, Geneva, 1958, 14, 24 (1958). A real spin-orbit depth of 33 MeV was used in these calculations. For charged particles, a square-well charge distribution was used.
[b] These values were selected somewhat arbitrarily to be similar to alpha-particle parameters, but with a deeper imaginary potential (and smaller particle size for d and Li⁶).

lated assuming $R = 1.2A^{1/3}$F. Values of $\bar{E}_{rot}$ so calculated varied between 1.7 MeV (for Cu⁶⁰ nuclei at 35 MeV of excitation) and 9.5 MeV (for Cu⁶⁰ nuclei at 70 MeV of excitation).

C. Computer Program

Two FORTRAN source programs were written for evaluation of Eq. (1). The first program was for the calculation of differential and integral probabilities for emitting a n, p, d, t, He³, and α particle as the first particle out, as well as the differential and integral probabilities for emitting a n, p, d, t, He³, or α particle as second particle following any given first particle; i.e., for each excitation energy of the compound nucleus, the kinetic-energy spectra, residual nuclear excitation spectra, and integrals of these values were calculated for 42 different permutations of one- and two-particle emission. Spectral points were calculated at 0.5-MeV intervals. In addition to the information cited above, the program also caused a tape to be written containing spectra of residual excitation energy for those spectra where further particle emission was possible.

The second program used the spectra of residual excitation provided by the first program to calculate n, p, and α emission probabilities and kinetic-energy spectra for emission of the third, fourth, and fifth particles.

A more detailed description of the programs has been given elsewhere[4,23]; however, the programs of this work have been improved to give normalized spectra, and to automatically prepare input for additional calculations where additional evaporation is possible.

An arbitrary decision must be made concerning calculated particle emission into the region $0 \leq E \leq \delta$, since machine calculations of this work consider no value of $E < (\delta + 0.5)$ MeV. Since there should be few states available in this region, we have assumed that there will be no particle emission into the region. An addi-

tional assumption was made concerning proton emission far below the Coulomb barrier. When the only two modes of deexcitation available are proton emission and gamma deexcitation, and where the kinetic energy available to the proton is ≤ 3.0 MeV (where proton inverse cross sections are decreasing exponentially to zero), we have assumed that proton emission does not compete with gamma emission. This assumption was shown to give consistently better agreement between calculated and experimental results in several other systems studied,[4,23] than did the assumption that γ-ray de-excitation cannot compete with particle emission. It has been predicted theoretically, and observed experimentally, that γ-ray de-excitation can compete with particle emission.[16,24] The argument here, however, is more one of tunneling probability than an angular-momentum argument as in Ref. 16.

III. RESULTS AND DISCUSSION

A. General Discussion of Calculations

The importance of considering the emission of particles other than neutrons, protons, and alpha particles in these calculations is emphasized in Fig. 1, in which the relative emission probabilities of n, p, d, t, He³, and α particles are shown as a function of excitation energy. The values of Fig. 1 were calculated for the first particle emitted in the decay of Cu⁶⁰ nuclei. The calculations of Figs. 1–3 were made without the rotational energy correction.

The relative importance of various permutations of calculated particle emission is shown in Figs. 2 and 3, where reactions leading to the production of Co⁵⁶ and Ni⁵⁶ are shown. The curves of Figs. 2 and 3 were calculated with Eqs. (1) and (2); no rotational energy has been subtracted. Sequence of emission is in the order indicated, i.e., $nppn$ implies order of emission was neutron, proton, proton, neutron. Calculated curves for which the first two particles were a neutron and

[23] M. Blann and G. Merkel, Nucl. Phys. (to be published).

[24] J. F. Mollenauer, Phys. Rev. 127, 867 (1962).

proton have been added, since the order of emission of the first two nucleons is unimportant, i.e., $\sigma_{np}=\sigma_{pn}$, at the excitation energies of these calculations. Verification of the latter statement may be seen in Fig. 1, where the neutron and proton emission probabilities have nearly zero slope at high excitations. The calculated dpn and pdn cross sections have also been summed to limit the number of curves shown in Fig. 3, as have the $dnp+ndp$, and $\mathrm{He^3}n+n\mathrm{He^3}$ excitation functions. Similar permutations of reaction products were necessarily calculated for all excitation functions displayed in Figs. 4–10. Their display was felt to be nonessential. All experimental cross sections shown in Figs. 4–9 have been normalized by division by the appropriate total nonelastic cross sections for Li⁶ ions on Fe⁵⁴ as calculated with the nuclear optical model.[14]

FIG. 3. Contributions of various calculated particle emission permutations leading to the formation of Co⁵⁶. Dotted excitation functions represent the emission permutations indicated; the solid curve is the sum over all possible reactions leading to the formation of Co⁵⁶.
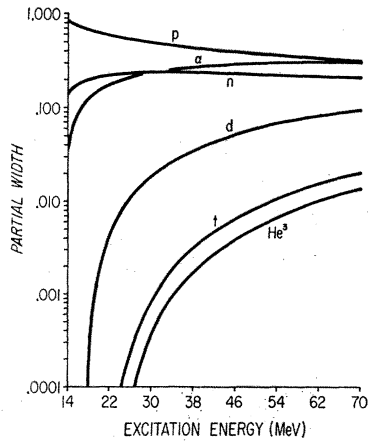
FIG. 1. Statistical-model prediction of the probability of emitting a n, p, d, t, He³, or α particle from an excited Cu⁶⁰ nucleus.

FIG. 4. Experimental and calculated excitation functions for the formation of Co⁵⁶ from Fe⁵⁴+Li⁶. The dashed curve represents the statistical theory prediction with no rotational energy correction, the dotted curve represents the statistical theory calculations with rotational energy shift. The solid curve has been drawn through the experimental points.

B. Comparison of Calculated and Measured Excitation Functions

As stated previously, two sets of calculations are presented for each experimental excitation function. The first set was calculated with no rotational energy correction, and is represented in Figs. 4–9 as dashed curves; the second set has had the ground-state energy shifted by the average rotational energy calculated with Eq. (5), and is represented by dotted curves. Experimental points have been joined by a solid curve. It should again be emphasized that the approximation made in using Eq. (6) is most easily justified for calculating excitation functions where multiple single-nucleon emission is the main contributor to total cross section (Figs. 4–7) and is most difficult to justify where α emission is significant (Figs. 8–9).

FIG. 2. Contributions of various calculated particle emission permutations leading to the formation of Ni⁵⁶. Dotted excitation functions represent the permutations indicated; the solid curve is the sum over all possible reactions leading to the formation of Ni⁵⁶. The curve labeled $npnn$ includes the $pnnn$ contribution.

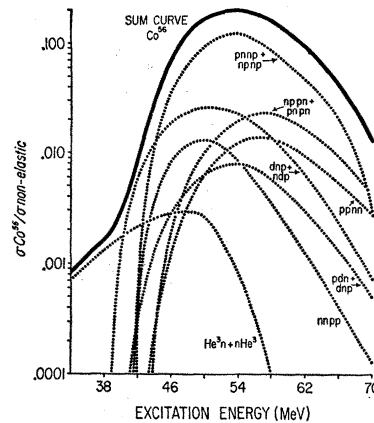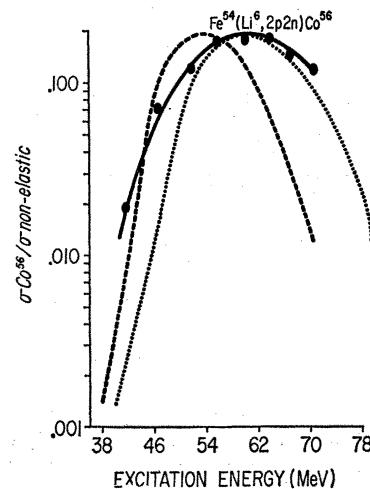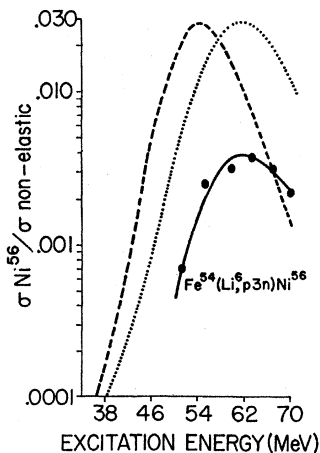FIG. 5. Experimental and calculated excitation functions for the formation of Ni^{56} from $Fe^{54}+Li^6$. The dashed curve represents the statistical theory prediction with no rotational energy correction, the dotted curve represents statistical theory prediction with rotational energy shift. The solid curve has been drawn through the experimental points.

Comparison of the two sets of calculated and experimental excitation functions of Figs. 4–8 yields the same general conclusions:

I. The excitation energies at which curves calculated with rotational energy corrections attain their maxima is in excellent agreement with the experimental values.

II. The widths of the above mentioned curves are also in good agreement with the experimental excitation functions.

III. The curves calculated with no rotational energy correction all attain their maxima at lower energies than the experimental excitation functions, and are all narrower than the experimental excitation functions.
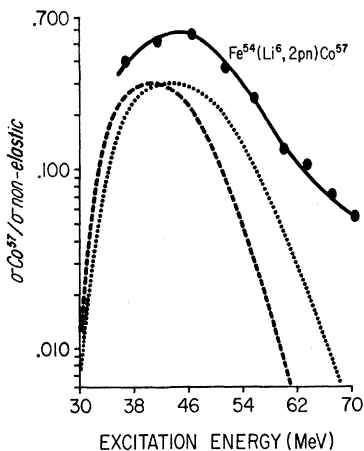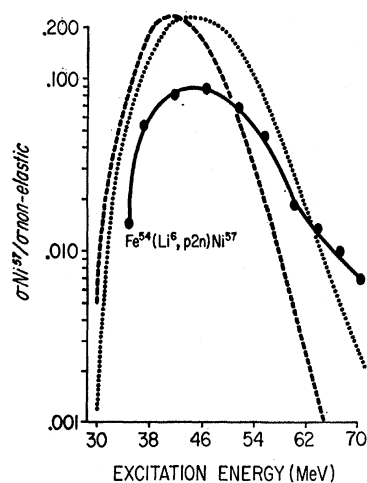
The excitation function for the production of Fe^{52}

FIG. 7. Experimental and calculated excitation functions for the formation of Ni^{57} from $Fe^{54}+Li^6$. The dashed curve represents the statistical theory prediction with no rotational energy correction, the dotted curve represents statistical theory prediction with rotational energy shift. The solid curve has been drawn through the experimental points.

(Fig. 9) would have to be measured at higher excitation energy before a significant comparison could be made with calculated values.

Figure 10 illustrates the success of the statistical theory with rotational energy correction. In Fig. 10 the experimental Ni^{58} $(d,\alpha)Co^{56}$ and Fe^{54} $(Li^6,2p2n)Co^{56}$ normalized excitation functions have been plotted from 14 to 70 MeV of excitation. The solid curve is the calculated excitation function. It may be seen that a single set of statistical theory parameters yields satisfactory agreement with experimental values over a wide range of excitation energies and reaction types. From the agreement between theory and experiment in Figs. 4–10 we
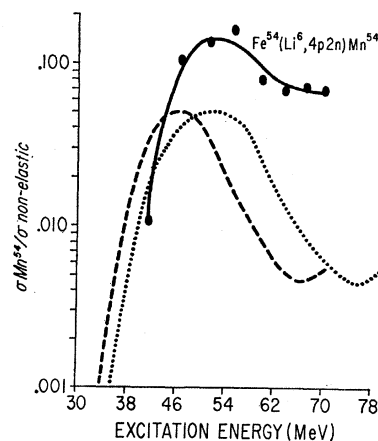

FIG. 6. Experimental and calculated excitation functions for the formation of Co^{57} from $Fe^{54}+Li^6$. The dashed curve represents the statistical theory prediction with no rotational energy correction, the dotted curve represents statistical theory prediction with rotational energy shift. The solid curve has been drawn through the experimental points.

FIG. 8. Experimental and calculated excitation functions for the formation of Mn^{54} from $Fe^{54}+Li^6$. The dashed curve represents the statistical theory prediction with no rotational energy correction, the dotted curve represents statistical theory prediction with rotational energy shift. The solid curve has been drawn through the experimental points. Energetic considerations require that one of the emitted particles be an α particle.
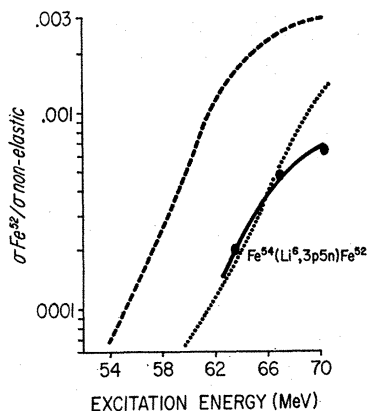
FIG. 9. Experimental and calculated excitation functions for the formation of Fe^{52} from $Fe^{54} + Li^6$. The dashed curve represents the statistical theory prediction with no rotational energy correction, the dotted curve represents statistical theory prediction with rotational energy shift. The solid curve has been drawn through the experimental points. Energetic considerations require that one of the emitted particles be an α particle.

conclude that the experimental excitation functions considered in this work are consistent with decay of a compound nucleus at statistical equilibrium.

C. Influence of Closed Shells on Nuclear Level Densities

As may be seen in Figs. 4–7, calculated cross sections are too high for nickel isotopes. The low experimental yields of nickel isotopes are therefore too low to be explained by the influence on level densities caused by the difference in neutron and proton binding energies. This conclusion is consistent with observations of another investigation in this region.[23] Results of the two investigations are summarized in Table II. The most obvious explanation of the anomalously low nickel yields appears to be the effect of the 28-neutron and 28-proton closed shells on the level densities of excited nuclei.
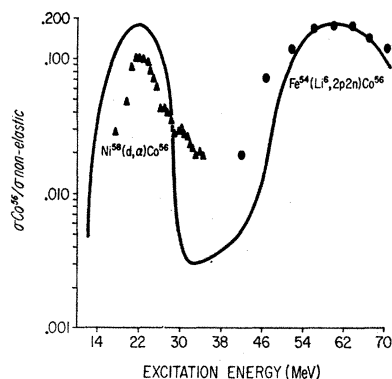

FIG. 10. Application of the statistical theory from 14 to 70 MeV of excitation. The triangles represent yields from the $Ni^{58}(d,\alpha)Co^{56}$ reaction; closed circles represent yields from the $Fe^{54}(Li^6,2p2n)Co^{56}$ reaction. The solid curve is the statistical theory prediction, calculated with a rotational energy correction to the excitation energy as in Eq. (6).

TABLE II. Summary of experimental and calculated excitation function ratios at maximum yield from this work and Refs. 5 and 23.

Reactions	Experimental ratio	Calculated ratio
$\dfrac{Ni^{58}(\alpha,\alpha p)Co^{57}}{Ni^{58}(\alpha,\alpha n)Ni^{57}}$	7.8	1.1[a]
$\dfrac{Fe^{54}(Li^6,2pn)Co^{57}}{Fe^{54}(Li^6,2np)Ni^{57}}$	6.6	1.3[b]
$\dfrac{Ni^{58}(\alpha,\alpha pn)Co^{56}}{Ni^{58}(\alpha,\alpha 2n)Ni^{56}}$	60	10.5[c]
$\dfrac{Fe^{54}(Li^6,2p2n)Co^{56}}{Fe^{54}(Li^6,p3n)Ni^{56}}$	57	7.1[b]

[a] From Ref. 23.
[b] From Ref. 5.
[c] Unpublished data (M. Blann).

IV. CONCLUSIONS

Experimental excitation functions discussed in this work have their maximum yields at higher excitation energies than those calculated with Eq. (2). If the excitation energy of the statistical theory calculations is decreased by the average rotational energy, the calculated curves attain their maxima at approximately the same excitation energy as the experimental curves. The widths of the excitation functions calculated with rotational energy correction are also in good agreement with experimental values. The agreement between calculated curves and experimental excitation functions leads us to conclude that the experimental results are consistent with statistical equilibrium persisting to 70 MeV of excitation, and probably higher in the region $A = 60$. It is also shown that the low yields of Ni isotopes are too small to be explained by the difference in neutron and proton binding energies. It is concluded, as in a previous investigation, that the low yields are due to the influence of the 28-nucleon shell on the level densities of Ni^{56} and Ni^{57}.

We wish, finally, to acknowledge that a treatment of rotational energy similar to that of this work was performed prior to this work by Stearns and Miller.[25]

[25] C. M. Stearns and J. M. Miller, Atomic Energy Commission Document NYO-10387, 1962 (unpublished).